MIT Open Access Articles

C. elegans MCM-4 is a general DNA replication and checkpoint component with an epidermis-specific requirement for growth and viability

Massachusetts Institute of Technology

C. elegans MCM-4 is a general DNA replication and checkpoint component with an epidermis-specific requirement for growth and viability

Jerome Korzelius [a,1], Inge The [a], Suzan Ruijtenberg [a], Vincent Portegijs [a], Huihong Xu [c],
H. Robert Horvitz [b], Sander van den Heuvel [a,*]

[a] Developmental Biology, Utrecht University, Padualaan 8, 3584 CH Utrecht, The Netherlands
[b] Howard Hughes Medical Institute, Department of Biology, Massachusetts Institute of Technology, Cambridge, MA, USA
[c] Department of Pathology and Laboratory Medicine, Boston University School of Medicine and Boston Medical Center, 670 Albany Street, Boston, MA, USA

ARTICLE INFO

ABSTRACT

DNA replication and its connection to M phase restraint are studied extensively at the level of single cells but rarely in the context of a developing animal. C. elegans lin-6 mutants lack DNA synthesis in postembryonic somatic cell lineages, while entry into mitosis continues. These mutants grow slowly and either die during larval development or develop into sterile adults. We found that lin-6 corresponds to mcm-4 and encodes an evolutionarily conserved component of the MCM2-7 pre-RC and replicative helicase complex. The MCM-4 protein is expressed in all dividing cells during embryonic and postembryonic development and associates with chromatin in late anaphase. Induction of cell cycle entry and differentiation continues in developing mcm-4 larvae, even in cells that went through abortive division. In contrast to somatic cells in mcm-4 mutants, the gonad continues DNA replication and cell division until late larval development. Expression of MCM-4 in the epidermis (also known as hypodermis) is sufficient to rescue the growth retardation and lethality of mcm-4 mutants. While the somatic gonad and germline show substantial ability to cope with lack of zygotic mcm-4 function, mcm-4 is specifically required in the epidermis for growth and survival of the whole organism. Thus, C. elegans mcm-4 has conserved functions in DNA replication and replication checkpoint control but also shows unexpected tissue-specific requirements.

Introduction

A crucial aspect of the cell division cycle is DNA replication, which takes place during the synthesis (S) phase of the cell cycle (Arias and Walter, 2007; Bell and Dutta, 2002). DNA replication must be highly accurate and tightly controlled to maintain genomic integrity over many rounds of cell division. A developmental context adds additional constraints on S-phase regulation. For instance, in meiosis M phases follow each other without intervening S phases, while in endoreduplication cycles, rounds of DNA replication continue in the absence of M phases. Nonetheless, during the division of most somatic cells, DNA duplication should happen once and only once, and M phase should not initiate until S phase is complete. Stalled replication forks and DNA damage activate a checkpoint that delays cell cycle progression (Ciccia and Elledge, 2010). Activation of this replication/damage checkpoint involves the Chk1 kinase and forms part of normal Drosophila and C. elegans development. Drosophila Chk1 (grapes) is required for decelerating embryonic cell cycles at the midblastula transition (Fogarty et al., 1997; Sibon et al., 1997), while the C. elegans ortholog chk-1 contributes to different cell cycle timing of early blastomeres (Brauchle et al., 2003). Thus, DNA replication and replication checkpoint control have developmental functions that go beyond the duplication of individual cells.

Studies of single-cell eukaryotes, Xenopus egg extracts and mammalian cells in culture have generated substantial insights in the process of DNA replication (Arias and Walter, 2007; Bell and Dutta, 2002). To accomplish the correct duplication of its DNA in each cell cycle, the cell treats the 'licensing' of the DNA for replication and the actual start of DNA replication as separate events. In the licensing phase of the cell cycle, pre-replication complexes (pre-RCs) are assembled at future origins of DNA replication. The sequential action of ORC1-6 proteins, Cdc6 and Cdt1 load the MCM2-7 DNA helicase onto the origins during late mitosis and early G1 (Bell and Dutta, 2002). The MCM2-7 complex is thought to act during S-phase as the helicase that unwinds the DNA at the replication origins (Aparicio et al., 1997; Labib et al., 2000; Pacek and Walter, 2004). At the onset of S phase, CDK (cyclin-dependent kinase) and DDK (Dbf-4 dependent Cdc7 kinase) activity control activation of the MCM2-7 helicase while at the same time preventing new recruitment of MCM2-7 complexes. This way, DNA synthesis is limited to a single round in each cell cycle (Nguyen et al., 2001; Petersen et al., 1999; Piatti et al., 1996; Schwob and Nasmyth, 1993).

Our understanding of the control of DNA replication in an organismal context is less advanced. However, important insights have been obtained from studies of, for instance, endoreduplication and gene amplification in *Drosophila* (Claycomb and Orr-Weaver, 2005; Lilly and Duronio, 2005). In addition, work from various researchers has demonstrated that conserved molecular modules regulate S-phase entry and DNA replication checkpoint responses in *C. elegans* (Kipreos, 2005; O'Neil and Rose, 2006; van den Heuvel, 2005). Several studies illustrate the potential for uncovering novel aspects of DNA replication control in *C. elegans*. For instance, analysis of DNA re-replication in *C. elegans* resulted in the discovery of the CUL-4/DDB-1 E3 ubiquitin ligase, which prevents origin re-firing and is conserved in mammals (Arias and Walter, 2006; Kim and Kipreos, 2007; Senga et al., 2006; Zhong et al., 2003). In addition, defects in DNA synthesis were found to cause lineage-specific delays in cell division, through a checkpoint mechanism that also contributes to the normal difference in timing of division between the anterior AB and posterior P1 blastomeres (Brauchle et al., 2003; Encalada et al., 2000). It is likely that genetic analyses of animal systems will reveal additional mechanisms that connect S-phase control to developmental processes.

In this study, we report the molecular and genetic characterization of the *C. elegans* gene *lin-6*. We show that *lin-6* mutant larvae maintain temporal expression of S-phase and differentiation genes, while the somatic cells are defective in DNA synthesis and lack the G2/M checkpoint that senses incomplete replication. Mapping and cloning revealed that *lin-6* is also known as *mcm-4* and encodes the *C. elegans* MCM4 ortholog, a member of the six-subunit MCM2-7 pre-RC and replicative helicase complex. Our results support a conserved function of *mcm-4* in replication licensing, DNA synthesis and the replication checkpoint. In addition, *mcm-4* is essential for normal larval growth and viability, which reflects a surprisingly specific MCM-4 requirement in the outermost epithelial cell layer known as hypodermis or epidermis.

Materials and methods

Strains and culturing

Strains were cultured on NGM plates seeded with *E. coli* OP50 according to standard protocol. Feeding RNAi was performed on NGM plates supplied with 50 μm/ml Ampicillin and 2 mM IPTG. Animals were synchronized by hypochlorite treatment and hatching eggs in M9 medium with 0.05% Tween-20. L1 larvae were then transferred to NGM plates with OP50 and allowed to develop for the appropriate amount of time. Experiments were conducted at 20 °C unless indicated otherwise. Strains used were: N2 Bristol wild-type, CB3475 *lin-6(e1466)/szT1[lon-2 (e678)]; +/szT1*, MT1442 *lin-6(e1466) dpy-5(e61)/szT1[lon-2(e678)]; +/ szT1*, JK2739 *lin-6(e1466) dpy-5(e61)/hT2[bli-4(e937) let-?(q782) qIs48]*, SV987 *cyd-1(he112) rol-1(e91)/mnC1; heIs30[Prnr-1::cyb-1DesBox::3X-Venus]*, SV1035 *mcm-4(e1466) dpy-5(e61)/szT1[lon-2(e678)]; +/szT1; heEx349[Pmcm-4::MCM-4::mCherry]*, SV1032 *lin-6(e1466) dpy-5(e61)/ szT1[lon-2(e678)]; +/szT1; heEx347[Prnr-1::cyb-1DesBox::3XVenus]*, SV1055 *mcm-4(e1466) dpy-5(e61)/szT1[lon-2(e678)]; +/szT1;heEx358 [Pelt-2::MCM-4::mCherry]*, SV1056 *mcm-4(e1466) dpy-5(e61)/szT1[lon-2(e678)]; +/szT1;heEx359[Pelt-2::MCM-4::mCherry]*, SV1057 *mcm-4 (e1466) dpy-5(e61)/szT1[lon-2(e678)]; +/szT1;heEx360[Pdpy-7:: MCM-4::mCherry]*, SV1058 *mcm-4(e1466) dpy-5(e61)/szT1[lon-2(e678)]; +/ szT1;heEx361[Pdpy-7::MCM-4::mCherry]*, SV1059 *mcm-4(e1466) dpy-5 (e61)/szT1[lon-2(e678)]; +/szT1;heEx362[sur-5::GFP;myo-2::TdTomato]*.

Molecular cloning of lin-6

Deficiencies *tDf3,* which includes *lin-6*, and *tDf4,* which does not include *lin-6*, were used to link the *lin-6(e1466)* mutation to the physical map. YACs from the region were used in transgenic rescue experiments and Y74C10 was observed to rescue the *lin-6* phenotype.

This ~330 kb YAC was labeled with γ^{32}P-ATP and used as a probe to isolate cDNAs from a *C. elegans* library. Forty-three cDNAs were identified and assigned to at most 9 different genes. RNA interference of one of these genes caused cell cycle defects that closely resembled those of *lin-6* mutants. One of the eight independent cDNAs for this gene (clone 6.10) was used as a probe to isolate genomic clones from a *C. elegans* phage library. Two of the identified clones partially rescued the *lin-6(e1466)* phenotype, suggesting that this genomic DNA includes the *lin-6* gene and that the cDNAs were derived from *lin-6*. The nucleotide sequences from four independent cDNAs were determined, and genomic DNA from wild-type and *e1466* animals was sequenced to determine the exon and intron sequences and nature of the mutation. All cDNAs contained sequences from 7 exons, a 3' poly(A) tract, and are predicted to encode the MCM-4 protein of 823 amino acids. This protein is likely full-length for three reasons: the first methionine is preceded by a stop three codons upstream, several cDNAs and ESTs start at about the same nucleotide and northern analysis of wild-type mRNA revealed a single transcript consistent with the size of the cDNA.

Reporters, transgenics and microscopy

MCM-4::mCherry (Pmcm-4::MCM-4::mCherry::mcm-4 3'UTR) was generated by amplifying a 5.7 kb fragment encoding MCM-4 and 2.4 kb of promoter sequence from genomic N2 DNA using Phusion polymerase (Finnzymes) and cloning this fragment into the pGEMT vector (Promega). Subsequently, the mCherry coding sequence (a kind gift of R. Tsien) together with the *unc-54* 3' UTR was amplified by PCR with Phusion and was fused in-frame with the *mcm-4* coding sequence in the pGEMT vector. The *unc-54* 3'UTR was replaced with the 650 bp *mcm-4* 3'UTR, which was amplified from genomic N2 DNA, to yield the MCM-4::mCherry reporter. Constructs of the MCM-4:: mCherry reporter with either the *mcm-4* or *unc-54* 3'UTR were injected into the MT1442 strain at a concentration of 30 ng/μl. *myo-2:: GFP* and *lin-48::GFP* were used as co-injection markers, respectively. The transgenes rescued *mcm-4(e1466)* larval development, resulting in adults that produced dead embryos. Both constructs gave similar expression patterns in four independent transgenic lines. *Pdpy-7:: MCM-4::mCherry* and *Pelt-2::MCM-4::mCherry* were created by replacing the *mcm-4* promoter from the *Pmcm-4::MCM-4::mCherry::mcm-4 3'UTR* construct by a 500 bp (*dpy-7*) or a 5 kb (*elt-2*) promoter fragment. Constructs were co-injected with *sur-5::GFP* (50 ng/μl) and *myo-2::TdTomato* (10 ng/μl) into the CB3475 or MT1442 strain. *Prnr:: CYB-1DesBox::3XVenus* was created by cloning a tandem *C. elegans*-optimized Venus (a kind gift of T. Ishihara, Kyushu University, Kyushu, Japan) in-frame with an N-terminal fragment of *C. elegans cyb-1* cyclin B1 (nucleotides 1–321). This CYB-1DesBox fragment contains a putative destruction box for APC-dependent degradation. The codon usage was altered (optimized) to prevent co-suppression of the endogenous *cyb-1* gene. CYB-1DesBox was expressed as a translational fusion with tripleVenus, controlled by the *rnr-1* ribonucleotide reductase promoter in the pVT501 vector (a kind gift of V. Ambros). Detailed cloning information and sequence maps are available upon request. This construct was injected into MT1442 *mcm-4(e1466) dpy-5(e61)/szT1[lon-2(e678)]; +/szT1*) at 40 ng/μl with *lin-48::TdTomato* as a co-injection marker. Transgenic lines were created by micro-injection as described (Mello et al., 1991). To examine reporter gene expression, animals were washed off the plates, anaesthetized with 10 mM Sodium Azide and mounted on slides with a 2% agar pad. Most images were taken with an Axioplan 2 microscope and Axiocam mRM camera (Zeiss Microscopy). Time-lapse images were acquired with a CSU-X1 Yokogawa spinning disk confocal system mounted on an inverted microscope (Nikon) and using an EMCCD camera (iXON DU-885, Andor Technology). Anterior is left, dorsal up in all figures. Scale bar 10 μm, unless otherwise indicated.

Immunostaining and antibodies

EdU (5-ethynyl-2′-deoxyuridine) labeling and staining were performed according to a protocol developed by S. Crittenden and J. Kimble using the Click-IT EdU Alexa Fluor 594 kit (Invitrogen). In short, MG1693 (Thy-deficient) bacteria were grown in 100 ml of minimal medium containing 20 mM EdU. Worms were fed on NGM + ampicillin plates with these bacteria for the appropriate time. For fixation, worms were freeze-cracked on poly-L-lysine coated slides in liquid nitrogen and subsequently immersed in methanol (5 min at −20 °C) and acetone (20 min at −20 °C). Slides were washed 1× in PBS with 0.1% Tween-20 and incubated with PBS + 0.1% Triton X-100 for better permeabilization. Slides were dried and the animals encircled with a PAP liquid blocker pen. The Click-IT reaction was subsequently performed on slides according to the manufacturer's instructions. Afterwards, slides were blocked using 10% donkey serum and 1% BSA and stained with monoclonal mouse anti-GFP (1:100, Sigma). Donkey anti-mouse FITC (Jackson Immunoresearch Laboratories) was used as a secondary antibody. Slides were mounted in Prolong Anti-Fade Gold (Invitrogen) supplied with 2 µg/ml DAPI. Propidium iodide and BrdU staining were performed as previously described (Boxem et al., 1999). Immunostaining of *C. elegans* embryos was performed as previously described (van der Voet et al., 2009).

Antibodies were raised against an MCM-4 internal 336 amino acid peptide (XhoI-BamHI fragment) supplied with an N-terminal 6xHis tag and purified from *E. coli* on Ni^{2+} beads. Anti-rabbit MCM-4 (Rabbit/Bleed 62-3) sera were either used crude (1:100, Fig. S4) or after affinity-purification with the same protein-fragment blotted onto nitrocellulose membranes (1:20, Fig. 6). Other primary antibodies used: anti-Nuclear Pore Complex mAB414 (Abcam, 1:100), anti-P-granule antibody K67 (Developmental Studies Hybridoma Bank, 1:2), anti-AJM-1 antibody MH27 (Developmental Studies Hybridoma Bank, 1:20), and rabbit anti-dsRed (Clontech, 1:100). Secondary antibodies used were: goat anti-mouse Alexa-488 (Invitrogen, 1:250), goat anti-rabbit Alexa-568 (Invitrogen, 1:250). Fluorescent images were taken with an Axioplan 2 microscope and Axiocam mRM camera (Zeiss Microscopy). Anterior is left, dorsal up in all figures. In both immunostaining and live imaging experiments, a minimum of $n = 10$ animals were examined for each treatment. Scale bar 10 µm, unless otherwise indicated.

Results

lin-6 mutants enter mitosis without DNA replication

The *lin-6(e1466)* mutation was identified in the first systematic search for mutants with defects in the normally invariant postembryonic cell lineages of *C. elegans* (*lin* mutants) (Horvitz and Sulston, 1980; Sulston and Horvitz, 1981). *lin-6(e1466)* mutant animals were reported to initiate mitosis while DNA replication was absent outside of the germline. This phenotype suggested a checkpoint defect and prompted us to investigate the cell cycle defects in *lin-6* mutants in more detail.

Heterozygous *lin-6(e1466)*/+ animals developed as normal (Fig. 1A and C and data not shown), indicating that the *lin-6(e1466)* allele is recessive. We generated *trans*-heterozygotes of *lin-6(e1466)* and the deficiency *tDf3*, which spans the entire *lin-6* locus, and found them indistinguishable in phenotype from homozygous *lin-6(e1466)* mutants (Table 1). Thus, *e1466* is probably a strong loss of function or null allele of *lin-6*. In the presence of maternal wild-type product, *lin-6(e1466)* homozygous animals completed embryogenesis and hatched as normal first-stage larva (L1). Starting in the first larval stage, cell divisions failed, yet the animals continued to grow at a rate that is reduced and more variable than that of wild-type animals (Figs. 1A–D and 7). The divisions of all postembryonic blast cells outside the gonad were defective and formed abnormally small nuclei (Fig. 1F, arrowhead). Some of these

nuclei remained in close contact, probably as a result of incomplete mitosis and cytokinesis, while others fully separated (Figs. 1A–F and 7C and D). Germline development was slow but frequently continued until the L4 stage. As a result, *lin-6* mutants that reached the adult stage generally had extensive gonads, with reflexed arms and sperm cells, but without oocytes (Fig. 1G). We examined the presence of germ-cell specific P-granules by immunohistochemistry (Strome and Wood, 1983). Gonads of *lin-6* animals showed extensive staining of P-granules, which demonstrates the proliferation of precursor germ cells during larval development (Fig. 1H). Thus, starting in the L1 stage, somatic blast cell undergo abnormal divisions in *lin-6(e1466)* larvae, while germline development continues until late larval development.

We used incorporation and immunohistochemical detection of the thymidine analogue BrdU as a sensitive assay for DNA synthesis. Wild-type animals grown in the presence of BrdU from 0 to 14 h of larval development incorporated BrdU in the postembryonic blast cell lineages (Fig. 1I). In *lin-6* mutants, only cells in the germline continued DNA replication (Fig. 1J). Occasionally, limited DNA synthesis could be detected in the blast cells that initiate postembryonic division soon after hatching. These cells include the neuroblasts QR and QL, the mesoblast M and the epidermal nuclei V5R and V5L (Fig. 1J, arrowhead and data not shown). We did not detect any BrdU incorporation in the precursor cells of the ventral nerve cord (P cells) (compare Fig. 1I and J). We used DIC microscopy to follow the development of progeny from heterozygous parents from the early L1 stage onward. Homozygous *lin-6* mutant larvae initiated postembryonic blast cell divisions at the same time as their heterozygous and wild-type siblings (data not shown). The 12 P precursor cells produced on average 27 ± 3.1 SD daughters, confirming that some even went through a second round of division in the absence of DNA replication. Together, these observations confirm that postembryonic somatic blast cells fail to replicate their DNA but initiate mitosis without delay in *lin-6* mutant animals.

lin-6 is required for the checkpoint that couples M phase entry to S-phase completion

Replication defects are expected to trigger a checkpoint that delays mitotic entry (Hook et al., 2007). Thus, it is remarkable that somatic cells in *lin-6* mutants enter mitosis at the normal time in the apparent absence of DNA replication. We considered two alternative explanations for this aspect of the Lin-6 phenotype: *lin-6* is required for DNA synthesis and also to activate the checkpoint that monitors completion of DNA replication, or alternatively, incomplete S phase cannot be sensed by a checkpoint in *C. elegans* larvae. To discriminate between these possibilities, we added the DNA replication inhibitor hydroxyurea (HU) to synchronously growing cultures of L1 animals. Subsequently, we fixed and stained animals for the mitosis-specific phosphorylated histone H3 Ser10 epitope (pH3S10) at various times of L1 development. Treatment of wild-type animals with HU delayed onset of mitosis for prolonged times (Fig. 2C, compare with A), demonstrating that initiation of mitosis is indeed dependent on the completion of DNA synthesis in *C. elegans*. Initiation of mitosis was not delayed in *lin-6* mutants treated with HU, indicating that mitotic entry is not coupled to DNA synthesis in these mutants (Fig. 2B and D). Thus, *lin-6* is required for DNA replication as well as for the checkpoint that restrains mitosis until completion of S phase.

lin-6 is not required for G1 progression and differentiation

Similar to *lin-6, cdk-4* Cdk4/6 and *cyd-1* cyclin D are also required for DNA synthesis during larval development (Boxem and van den Heuvel, 2001; Park and Krause, 1999). Postembryonic blast cells in *cdk-4* and *cyd-1* mutants arrest in G1 and do not activate the S-phase transcriptional reporter *rnr-1::GFP* (Boxem and van den Heuvel, 2001). We observed *rnr-1::GFP* expression in *lin-6* larvae but also
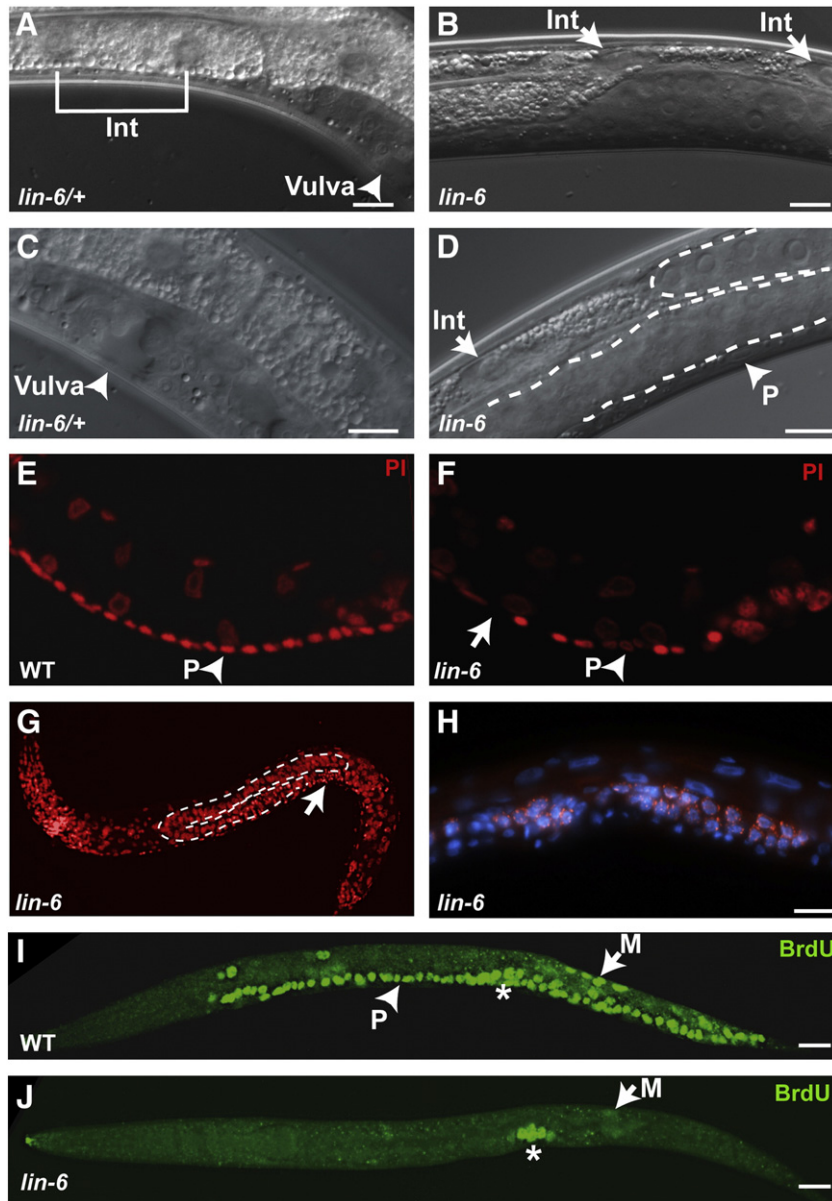
Fig. 1. *lin-6* mutant animals are defective in DNA replication and cell division. A–D: Differential interference contrast (DIC) microscopy images of *lin-6(e1466)* heterozygous larvae (A,C) and *lin-6(e1466)* homozygous mutants (B,D). *lin-6/+* larvae have normal cell divisions. Indicated are P cell descendants that form the vulva (A,C, arrowheads) and an intestinal cell after nuclear division (A, bracket). In contrast, *lin-6(e1466)* homozygous mutant animals lack postembryonic cell division in these tissues (B,D, arrows and arrowhead). Note the significant size of the gonad in the *lin-6* homozygous larva (D, gonad outlined with dotted line). E,F: DNA staining with propidium iodide (PI, red) illustrates division defects of the ventral cord precursor cells P in late L1 larvae. Descendants of the P cells fill the ventral cord in the wild type (E, arrow), while in the *lin-6(e1466)* mutant (F) defective P cell divisions create gaps (arrow) and small fragmented nuclei (arrowhead). G,H: The somatic gonad and germline continue DNA synthesis and considerable numbers of cell divisions during larval development of *lin-6(e1466)* mutants. (G) DNA stained with PI (red), the dashed line outlines a gonadal arm. Note the presence of sperm in the spermatheca (arrow). (H) Precursor germ cells are visualized by immunostaining of P-granules (red dots) in a L3-stage larva, DNA is stained with DAPI (blue). I,J: Detection of DNA replication. L1 larvae grown in the presence of the thymidine analogue BrdU from 0 to 14 h of larval development followed by anti-BrdU staining. (I) BrdU incorporation in a wild-type animal demonstrates DNA replication in various postembryonic lineages. Labeled cells include the descendants of the P cells (P, arrowhead) and mesoblast (M, arrow). (J) *lin-6* mutant larva, which shows postembryonic DNA replication only in the gonad (asterisk). Descendants of the Mesoblast (arrow), the V5 seam cells and Q neuroblasts (not visible) occasionally show limited DNA replication. Anterior is left, dorsal up in all figures. Scale bar, 10 μm.

quite frequently in starvation-arrested L1 larvae of the *rnr-1::GFP* control strain (data not shown). The latter observation indicates that fluorescence might result from ectopic expression of the *rnr-1::GFP* transgene or from GFP lingering from previous divisions. To create a more reliable marker for the G1/S transition, we fused a CYB-1 cyclin B1 N-terminal fragment (CYB-1DesBox), which directs APC/C-dependent protein degradation in mitosis, in-frame with triple Venus (3XVenus) and expressed this translational fusion protein from the *rnr-1* promoter (see Materials and methods). This *Prnr-1::CYB-1DesBox3XVenus* reporter is highly specific for cells in division, as fluorescence appeared during S phase, accumulated in the presence of

HU and disappeared at the time of M phase completion or soon thereafter. Again, wild-type and *lin-6(e1466)* L1 larvae expressed this S-phase reporter with similar temporal and spatial control, while the reporter was not induced in *cyd-1(he112)* mutant larvae (Fig. 3). We conclude that cells progress through the G1/S transition in *lin-6* mutants, yet fail to replicate their DNA.

Interestingly, *CYB-1DesBox3XVenus* expression disappeared more slowly in *lin-6* mutants than in wild-type animals (Fig. S1). As postembryonic blast cells in *lin-6* mutants enter mitosis at the appropriate time, based on the timing of nuclear envelope breakdown, the prolonged presence of CYB-1DesBox3XVenus likely indicates a delay

Table 1

Total progeny from four crosses, each between a single *lin-6(e1466)/+* male and *lin-6(e1466)/dpy-5(e61)* or *tDf3/dpy-5(e61)* hermaphrodite. For both types of crosses, approximately one quarter of the progeny were Stu (Sterile, Thin and Uncoordinated). Such animals develop slowly, vary in size and either arrest at a late larval molt or live as Stu adults. Right column: The total number of propidium iodide stained nuclei in the somatic gonad and germline was counted in five adults of each genotype.

Genotype crosses (n = 4)	Progeny phenotype			Gonad cell count
	Emb (n)	Stu (n)	WT (n)	
lin-6/+ X lin-6/+	0.9% (12)	25.8% (332)	73.3% (943)	122 ± 19, sperm 72 ± 54
lin-6/+ X lin-6(Df)/+	1.0% (14)	23.2% (313)	75.8% (1023)	131 ± 18, sperm 83 ± 57

in exit from mitosis. *Prnr-1::CYB-1DesBox3XVenus* was also detected at later times of development, in particular in the epithelial lateral seam cells and posterior daughters of the P (Pn.p) cells (data not shown). This expression cannot be explained by perdurance of the fluorochrome and indicates that cells continue their program of cell cycle entry, even when previous divisions failed.

In addition, induction of differentiation also continued in the absence of DNA replication. For instance, the formation of incomplete adult alae in part of the animals indicates completion of epithelial differentiation. Previous dye-filling studies demonstrated that *lin-6* mutants miss the PDE ciliary neuron in the postdeirids, a lateral neuronal structure formed during the first larval stage from posterior descendants of the V5 seam cells (Sulston and Horvitz, 1981). We introduced the *Pdat-1::GFP* transgene in the *lin-6(e1466)* background as a reporter for PDE cell fate determination (Nass et al., 2002). Expression of this transgene was seen in 20/20 *lin-6* animals assayed at the L4 larval stage (Fig. S2). Division of the precursor cells of the postdeirid was defective in *lin-6* mutants (Fig. S2, arrow), which probably prevents formation of a functional PDE ciliary neuron (Sulston and Horvitz, 1981). However, the *Pdat-1::GFP*-positive neurons sometimes formed axonal projections in *lin-6* animals that look similar to the projections seen in wild-type *Pdat-1::GFP*-positive neurons. These data suggest that cell type specification and differentiation can continue extensively in developing *lin-6* larvae even in cells that underwent aberrant division.

lin-6 encodes the MCM4 subunit of the MCM2-7 replication pre-initiation complex

We cloned the *lin-6* gene through a combination of genetic mapping and yeast artificial chromosome (YAC) rescue (see Materials and methods, Fig. S3A). Conceptual translation of *lin-6* cDNAs predicted a protein of 823 amino acids (Fig. S3B). Analysis of the corresponding DNA sequences in *lin-6(e1466)* revealed a G:C-to-A:T transition, which is predicted to change the Gln88 codon to an amber stop codon. Termination of translation this early is likely to result in strong or complete inactivation of LIN-6 function, in agreement with the genetic data for *lin-6(e1466)* (Table 1). The predicted function of the LIN-6 protein matches the loss-of-function phenotype: BLAST searches revealed that *lin-6* encodes an MCM family member, sharing

54% amino acid identity with human and *Xenopus laevis* MCM4 (Fig. S3C). First discovered in yeast, the MCM genes are essential for DNA replication in all eukaryotes studied (Bell and Dutta, 2002). Six different genes of this family, MCM2 to 7, are present in *S. cerevisiae*, and a single member of each subfamily appears to be conserved in other eukaryotes. The six MCM proteins form a hexameric complex, which licenses origins for DNA replication as a critical component of the DNA replication pre-initiation complex and acts as the replicative helicase during DNA replication. Because of the high degree of conservation, the *C. elegans* genome project already assigned the name *mcm-4* to the *lin-6* gene defined by mutation. We propose to adopt *mcm-4* as the common name and will use this name throughout the rest of this manuscript.

The replication pre-initiation complex is needed to restrain M phase

Analysis of the *mcm-4(RNAi)* phenotype further confirmed the double function of *mcm-4* in DNA synthesis and activation of a replication checkpoint that inhibits progression into mitosis. Previous studies showed that replication defects delay progression through the cell cycle of early blastomeres (Encalada et al., 2000), through activation of an *atl-1* ATR-dependent checkpoint pathway (Brauchle et al., 2003). In agreement with these studies, we found that inhibition of DNA replication by exposing adults to the ribonucleotide reductase inhibitor HU (100 mM) or *rnr-1* RNAi resulted in delayed mitotic entry in the one-cell embryo (Fig. 4A). Following the delay, spindle duplication continued without chromosome segregation, and the DNA remained present in the center of the embryo as a single or two separate masses (derived from the paternal and maternal pronucleus) in 49/50 embryos (Fig. 4D", compare to 4B", Fig. S4C, arrows). In contrast, mitotic entry was not delayed after *mcm-4* RNAi (Fig. 4A and C). The DNA was segregated to opposite poles and cycles of chromosome segregation followed by cell division continued, thereby reducing the amount of DNA in each blastomere (Fig. S4B, compare to DNA staining of polar bodies (arrowheads)). The DNA became fragmented (50/50 embryos, compared to none in the wild-type control), and ultimately these *mcm-4(RNAi)* embryos arrested with up to 30 nuclei and very little DNA in each nucleus (Fig. 6B).

RNAi of *mcm-4* substantially decreased the delay induced by *rnr-1* inhibition (Fig. 4A), further supporting that *mcm-4* is required for the
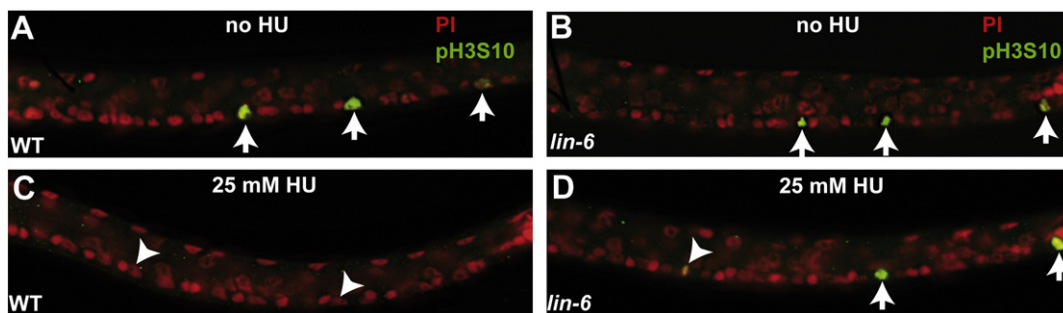
Fig. 2. Absence of a replication checkpoint response in *lin-6* mutants. Wild-type (A) and *lin-6* mutant (B) larvae at 10 h of L1 development contain mitotic P cells in the ventral cord, which stain positive for the mitosis-specific histone H3 phospho-Ser10 epitope (pH3S10) (A,B, arrows). C: Wild-type animal treated with the DNA-replication inhibitor hydroxyurea (HU). P cells have migrated into the ventral cord but remain phospho-H3S10 negative, indicating that cells arrest before mitosis (arrowheads). D: In the HU-treated *lin-6* animal, P cells failed to arrest before mitosis and show phospho-H3S10 positive staining (arrows) and a metaphase plate (arrowhead).
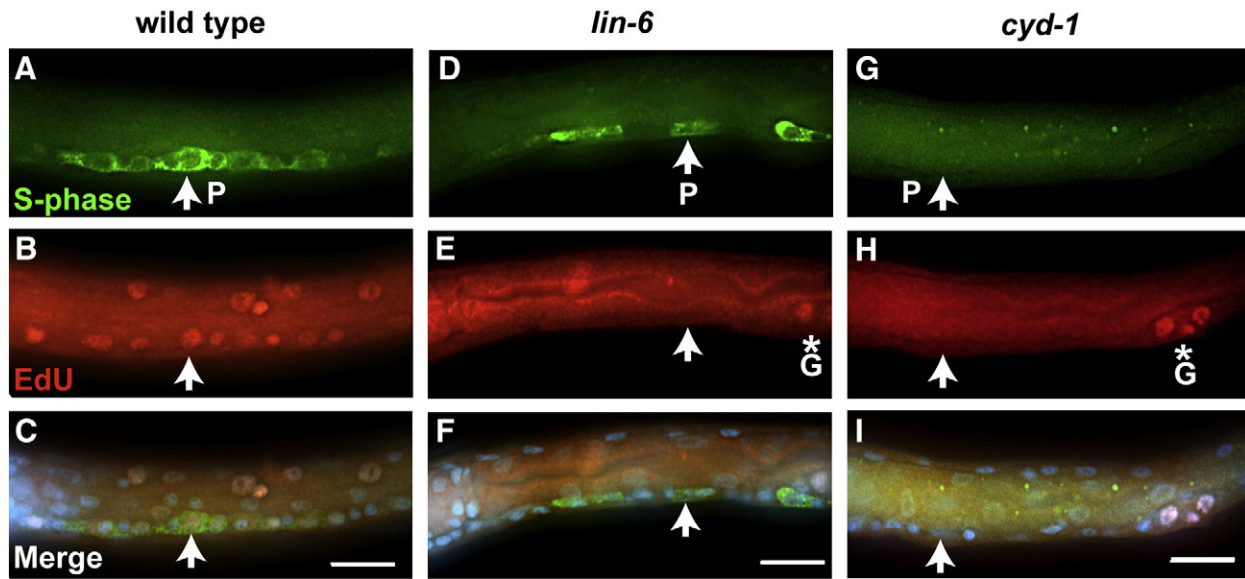
Fig. 3. Cells progress through the G1/S transition in *lin-6* mutants. Wild-type (left. A–C), *lin-6(e1466)* (middle, D–F) and *cyd-1(he112)* (right, G–I) mid-L1 larvae examined for S-phase induction and DNA synthesis. A,D,G: Immunostaining of Venus indicates expression of the S-phase reporter *Prnr::CYB-1Desbox::3XVenus* (see Materials and methods). P cells express Venus (green, arrow) in the wild type and *lin-6* mutant, but not in the *cyd-1* larva. B,E,H: Incorporation and staining of the thymidine analogue EdU reveals DNA synthesis. P cells (B, arrow) and other cells replicate DNA in the wild-type L1, while *lin-6* and *cyd-1* larvae show DNA synthesis only in the gonad (marked with asterisks). C,F,I: Merged images of anti-GFP(Venus), EdU and DNA staining with DAPI.

S-phase checkpoint that delays M-phase entry. However, *mcm-4 (RNAi)* was not fully epistatic to *rnr-1* inhibition, which indicates either residual *mcm-4* function or an *mcm-4* independent partial delay (Fig. 4A and E). RNAi of *mcm-5*, which encodes another MCM subunit, resulted in a phenotype similar to that of *mcm-4* (48/50 embryos). Genome fragmentation has also been reported for *cdt-1(RNAi)* and *cdc-6(RNAi)* embryos (Kim et al., 2007; Zhong et al., 2003). In contrast, inhibition of *div-1*, which encodes the DNA polymerase α primase B-subunit, resembled *rnr-1* inactivation and triggered mitotic delay (Encalada et al., 2000). We conclude that the MCM replicative helicase, which forms part of the DNA replication pre-initiation complex, is required for both DNA synthesis and the delay of cell cycle progression when replication is incomplete.

MCM-4 shows cell cycle-dependent expression and localization

How cells commit to and withdraw from the division cycle are important developmental questions. As a subunit of the DNA replication pre-initiation complex, MCM-4 should be present at the time of S-phase onset. Moreover, replication licensing is separated in time from activation of origin firing at G1/S, and as such MCM-4 might be expressed well before S phase or even remain present at the end of mitosis. To examine the temporal and spatial expression of MCM-4, we created an *MCM-4::mCherry* reporter construct and generated antibodies that recognize MCM-4.

The reporter transgene contains 2.4 kb of genomic DNA upstream of the predicted ATG translation initiation codon, the predicted *mcm-4* exon and intron sequences, and 650 bp downstream of the stop codon, including the predicted poly(A) signal. Coding sequences for mCherry were inserted just before the termination of the *mcm-4* open reading frame (see Materials and methods). Expression of this combined promoter and C-terminal translational fusion construct rescued the *mcm-4(e1466)* mutation. Specifically, *mcm-4(e1466)* animals with an extrachromosomal *Pmcm-4::MCM-4::mCherry* array appeared healthy and viable and showed normal cell division in the ventral cord, intestine and seam, formed a normal vulva and occasionally produced a few embryos (data not shown). Moreover, single copy integration of this *mcm-4::mCherry* transgene fully rescued the *mcm-4(e1466)* embryonic and postembryonic defects

(JK and SvdH, manuscript in preparation). As MCM-4::mCherry functionally substitutes for MCM-4, its expression and localization likely resembles the endogenous protein.

We did not detect MCM-4::mCherry in starvation-arrested L1 animals. However, expression was specifically induced in all postembryonic blast cell lineages well before mitotic entry, at the expected time of S-phase induction (Fig. 5A–H). The fusion protein localized to the cell nucleus until degradation of the nuclear envelope in prometaphase, at which point MCM-4 became diffusely localized through the cell. This diffuse localization indicates that MCM-4 is not chromatin-associated in mitosis (Fig. 5H, arrow). MCM-4::mCherry did not disappear upon completion of mitosis but was segregated to both daughter cells. Even cells that permanently withdrew from cell division, such as the motor neurons of the ventral nerve cord, initially retained MCM-4::mCherry expression (data not shown). However, this expression subsequently disappeared in differentiated cells as well as in cells that temporarily arrested cell division, such as the Pn.p vulval precursor cells in the ventral cord. These experiments indicate that *mcm-4* is transcriptionally activated at approximately the time of G1/S transition and that MCM-4 protein is segregated to both daughter cells in mitosis.

Detection of endogenous MCM-4 confirmed these observations. We generated rabbit polyclonal antibodies against an extended C-terminal MCM-4 fragment as well as mouse polyclonal antibodies that recognized an N-terminal domain. Antisera directed against either fragment recognized a protein with an apparent MW of ± 105 kD in total worm lysates (Fig. 6D and data not shown). This protein is likely MCM-4, based on its MW and absence in *mcm-4(e1466)* mutants, which contain an early nonsense mutation. We found MCM-4 expressed in dividing cells during all stages of development in wild-type animals. Embryos showed the highest levels of MCM-4 expression, in agreement with the fact that more than half of the somatic cells are formed during embryogenesis (Fig. 6D, lane 1). Interestingly, MCM-4 was reduced but clearly detectable in developmentally arrested L1 animals that hatched in the absence of food (Fig. 6D, lane 2). Even dauer larvae that had been arrested in cell division for 2 weeks still contained detectable MCM-4 protein levels (Fig. 6D, lane 7). These results suggest that a pool of MCM-4 is retained during prolonged periods of quiescence, so that MCM-4
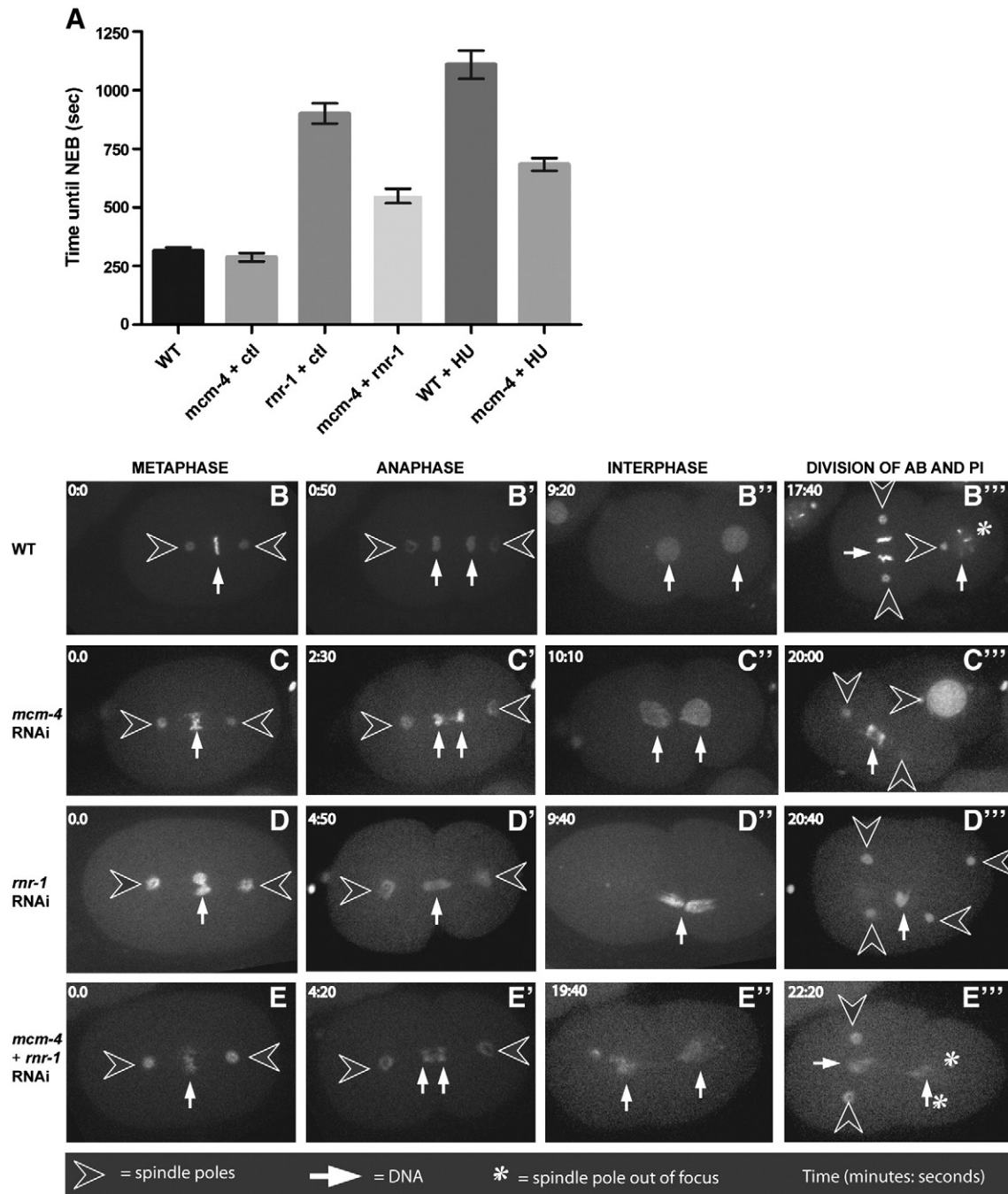
Fig. 4. *mcm-4(RNAi)* embryos lack DNA replication yet continue mitotic DNA segregation. A: Inhibition of *mcm-4* by RNAi does not delay mitotic entry and relieves the checkpoint induced by *rnr-1* inhibition. RNR-1 inhibition by RNAi or exposure of adults to HU (100 mM, 2–4 h) substantially delays mitotic entry (approximately 10–13 min, respectively). Combination with *mcm-4* knockdown diminishes this delay, which further indicates contribution of MCM-4 in an S-phase checkpoint over mitotic entry. Time indicates seconds between meeting of the maternal and paternal pronucleus in the posterior and nuclear envelope breakdown (NEB). Migration of the maternal pronucleus to the posterior is also delayed after *rnr-1* inhibition (not included). For proper comparison with *rnr-1 mcm-4* double RNAi, control (ctl: *gpd-2*) dsRNA was added to the *mcm-4* and *rnr-1* injection mix. B–E: Images from time-lapse spinning disk confocal microscopy illustrate that chromosome segregation continues in the absence of *mcm-4* (C C'''), but not after inhibition of *rnr-1* (D–D'''). Note that the zygotic DNA remains present in the center of the embryo, independent of the spindle and cell division (arrows, D' and D'').

might function in the re-initiation of DNA synthesis when conditions improve.

Immunostaining of wild-type animals for MCM-4 showed strong nuclear staining in the gonad, embryos and postembryonic lineages (Fig. 6A and C, Fig. S5). This staining was MCM-4-specific, as RNAi of *mcm-4* eliminated the nuclear signal in the germline and embryos, and *mcm-4(e1466)* larvae did not shown staining (Fig. 6B and data not shown). MCM-4 was detectable in sperm and accumulated during oocyte maturation in the nucleus but did not show overlap with the condensed chromosomes in diakinesis of meiotic prophase (Fig. S5 and data not shown). MCM-4 was not chromatin-associated during Meiosis I of the fertilized oocyte, and the first polar body did not contain MCM-4 (Fig. 6A). This finding is consistent with the absence of S phase between Meiosis I and -II. The second polar body and maternal pronucleus received some MCM-4. Subsequently, embryonic cells in interphase showed strong nuclear staining (Fig. 6A, Fig. S5 left panel). In prophase, MCM-4 localization did not overlap with the condensing chromosomes (Fig. 6A, Fig. S5). Upon nuclear envelope degradation, MCM-4 became diffusely localized throughout the cell and clearly did not co-localize with the metaphase-aligned chromosomes (Fig. 6A, arrowhead). MCM-
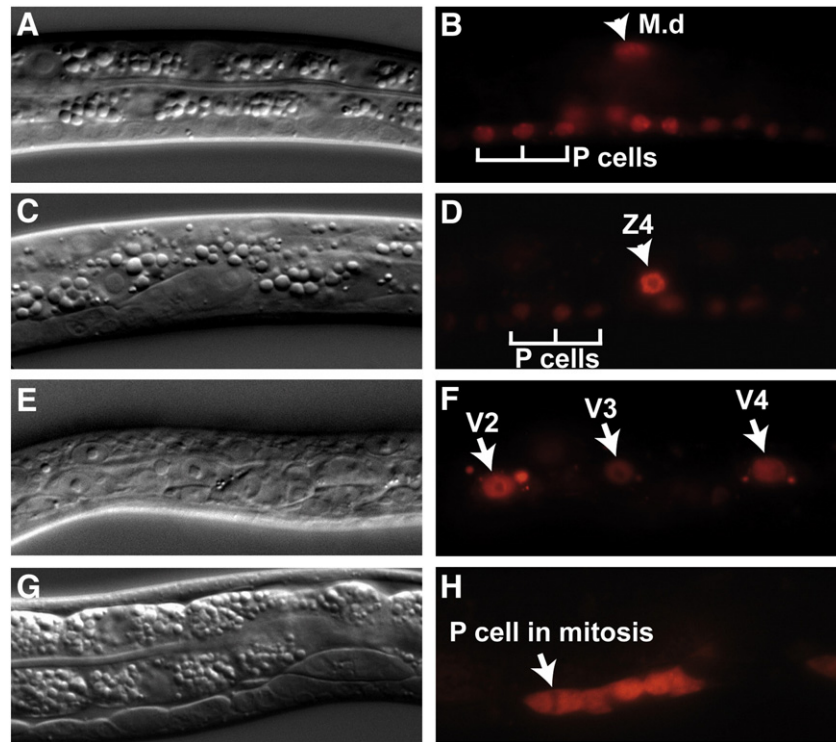
Fig. 5. The MCM-4::mCherry reporter marks cells in the division cycle. DIC (A,C,E,G) and fluorescence microscopy images (B,D,F,H) of L1 larvae carrying a *Pmcm-4::MCM-4::mCherry* expression construct (see Materials and methods). This transgene rescues the *mcm-4(e1466)* mutant and is highly expressed in proliferating postembryonic blast cells, including P cells (A–D, brackets, G,H), M cell descendants (A,B, arrowhead), the somatic gonad precursors (C,D, arrowhead) and V cells (E,F, arrows). MCM-4::mCherry is nuclear in interphase and absent from the DNA in metaphase (G,H, arrow), resembling the expression pattern as detected by antibody staining for MCM-4 (Fig. 6).

4 remained cytoplasmic at the onset of anaphase; however, chromatin association became apparent in late anaphase (Fig. 6A, Fig. S5A, C, and E, compare arrows with arrowheads). These data show that chromosome association of MCM-4 is tightly controlled, consistent with origin licensing taking place at the end of mitosis and disappearing during S phase.

Similar observations were made during larval divisions. Matching the MCM-4::mCherry reporter, endogenous MCM-4 expression was detectable prior to and during mitosis (Fig. 6C). Staining of synchronized L1 animals revealed the timing of MCM-4 expression, which in general preceded mitosis by 1–2 h. After 5 h of L1 development at 20 °C, MCM-4 immunostaining was predominantly detected in the epithelial seam cells, Q neuroblast daughters and gonad primordium. The somatic gonad precursor cells Z1 and Z4 showed nuclear staining, while the mitotically arrested germline precursor cells Z2 and Z3 showed diffuse cytoplasmic staining. At 6 hours of L1 development, the mesoblast (M) also stained strongly as well as the most anterior ventral cord precursors cells (W, P1 and P2). Subsequently at 7 h, additional P cells showed nuclear MCM-4 expression, which became apparent prior to migration of the nucleus into the ventral nerve cord (data not shown). At 8 h of L1 development, the intestinal nuclei showed MCM-4 expression (Fig. 6C), which preceded nuclear division by at least 4 h. At subsequent time points, daughter cells that continued division, such as the Pn.a and M descendants, retained strong nuclear staining. L2 animals stained at 16 h of larval development showed strong MCM-4 expression in the gonad, the H1.a, H2.p, V1-6.p and T.ap seam cells and, weakly, the intestinal nuclei (data not shown).

Importantly, MCM-4 staining did not overlap with DNA in prophase and metaphase, while in late anaphase co-localization with the chromosomes was clearly detectable (Fig. 6C). Similar to our observations with the *MCM-4::mCherry* reporter, we could not detect any asymmetry in MCM-4 segregation. Thus, even if only one daughter cell continued cell division, both daughters received a

similar amount of MCM-4 in mitosis. Furthermore, the MCM-4 protein became undetectable during quiescence, i.e. the P3.p-P8.p daughter cells that resume DNA replication in the L3 stage did not show detectable expression in the L2 stage. Altogether, our reporter gene and antibody staining analysis show that MCM-4 is dynamically expressed and localized during larval development as well as during different phases of the cell cycle. The strong induction of MCM-4 in cells that re-enter the cell cycle after quiescence suggests that MCM-4 expressed in G1/S can contribute origin-licensing and/or replicative helicase activity.

MCM-4 is required in the epidermis for organismal growth and viability

How cell division is coordinated with organismal growth is an important question in developmental biology. *mcm-4* mutants grow slowly and remain smaller and slimmer than wild-type animals (Fig. 7A and B). In addition, *mcm-4* mutants quite frequently arrest at the larval molts and subsequently die. *mcm-4* mutant larvae that were synchronized at hatching and subsequently were allowed to develop for 120 h had a 12% lethality rate (n = 97), while the wild-type and heterozygous *mcm-4(e1466)/+* siblings all developed into healthy gravid adults (n = 300). In contrast, mutations in *cyd-1* or *cdk-4* cause slow growth without associated lethality. As *cyd-1* and *mcm-4* mutants both fail to replicate DNA in postembryonic somatic cells, we assumed that DNA replication is needed for normal growth, while the lack of an S-phase checkpoint in *mcm-4* mutants probably underlies the lethality. To examine in which cell type *mcm-4* is required to promote growth and viability, we expressed *mcm-4* specifically in the epidermis or intestine. These two tissues go through endoreduplication cycles, which have been implicated in cellular growth, during larval development (Hedgecock and White, 1985; for review see Edgar and Orr-Weaver, 2001). Furthermore, the larval lethality of *mcm-4* mutants seemed to coincide with a molting defect, which suggested a requirement for MCM-4 function in the epidermis.
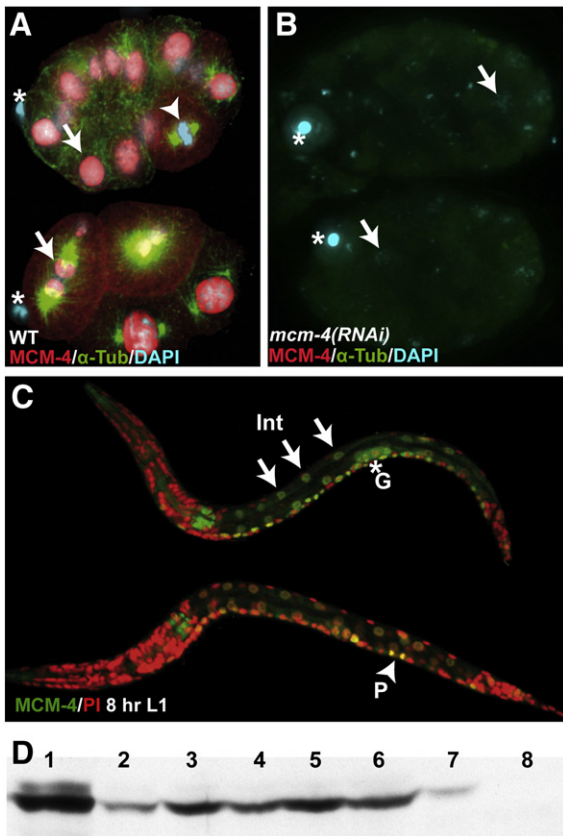
Fig. 6. MCM-4 is dynamically localized at different stages of the cell cycle and is expressed at different levels during development. A: Early *C. elegans* embryos stained for MCM-4 (red), α-tubulin (green), and DNA (DAPI, blue). MCM-4 is present in the nucleus in interphase (A, top arrow), does not co-localize with DNA in metaphase (A, arrowhead), but overlaps with chromatin in late anaphase (A, bottom arrow). B: MCM-4 staining is absent in *mcm-4(RNAi)*-treated embryos (B, arrows mark fragmented DNA). C: L1-stage larvae at 8 h of L1 development, immunostained for MCM-4, DNA visualized with propidium iodide. MCM-4 is visible in the intestinal nuclei (Int, arrows), nuclei and cytoplasm of the gonadal precursors (G, asterisk), and P cells in the ventral cord (P, arrowhead). MCM-4 does not overlap with DNA in metaphase but co-localizes with DNA in late anaphase. D: Western blot showing MCM-4 protein levels at different developmental stages. Lane 1: Embryos, 2: Starved L1, 3: L2, 4: L4, 5: L4, 6: Adults, 7: Dauer larvae, 8: *lin-6* mutants. Levels are highest in embryos and lowest in developmentally arrested starved L1 larvae and Dauer larvae.

Expression of MCM-4::mCherry under the control of the intestine specific *elt-2* promoter (Hawkins and McGhee, 1995) restored intestinal nuclear divisions and endoreduplication cycles in *mcm-4* animals (Fig. S6). This result confirms that *mcm-4* acts cell-autonomously in DNA synthesis and endoreduplication cycles. However, expression of MCM-4::mCherry in the intestine did not rescue the size or lethality of the *mcm-4* mutants. In contrast, expression of MCM-4::mCherry from the epidermal *dpy-7* promoter did rescue the growth and viability of *mcm-4(e1466)* mutant larvae. Control *mcm-4* transgenic animals expressing the *sur-5::GFP* marker without the *Pdpy-7::MCM-4::mCherry* rescue construct contained few epidermal nuclei (Fig. 7C, arrows). Such nuclei were often small and fragmented, probably because of aberrant mitosis without DNA replication (Fig. 7D, arrowheads, compare with Fig. 1F). Staining with MH27 antibodies, which recognize the apical junction-localized AJM-1 protein in *C. elegans* epithelia (Francis and Waterston, 1991), demonstrated that the structure of the seam cells in the worm epidermis is abnormal in *mcm-4(e1466)* animals (Fig. S7B). We noticed that transgenic *mcm-4(e1466)/+* animals with a *Pdpy-7:: MCM-4::mCherry* extrachromosomal array produced few animals with a typical Mcm-4 phenotype. However, sterile animals with a vulval protrusion (Pvl) were present that together with the Mcm-4

larvae formed approximately 1/4 (17/59) of the offspring. Examination of mCherry fluorescence revealed that the sterile Pvl animals all carried the extrachromosomal array, while the Mcm-4 animals had lost the array. Thus, expression of the *Pdpy-7::MCM-4::mCherry* transgene substantially rescues the Mcm-4 phenotype. We observed complete rescue of the small body length and width of the *mcm-4* mutants (Fig. 7B and data not shown). Moreover, Pvl animals carrying the *Pdpy-7::MCM-4::mCherry* transgene did not arrest during molting but developed into healthy, but sterile adults (n = 124 transgenic animals examined). Furthermore, the *Pdpy-7::MCM-4::mCherry* transgene restored cell division of the epidermal seam cells (Fig. 7E) as well as the structure of the seam cells in *mcm-4(e1466)* mutants (Fig. S7C). We also noticed some rescue of cell division of the epithelial posterior P cell descendants, consistent with data suggesting *dpy-7* promoter activity in the Pn.p cells (A. Saffer and H.R. Horvitz, personal communication). Other tissues, such as the intestine and gonad, developed as in *mcm-4* mutants and the transgenic animals were fully sterile. These data indicate that *mcm-4* function in the epidermis is sufficient to restore normal growth and viability in *mcm-4* mutant animals.

Discussion

Studies of simple animals such as *C. elegans* allow for a functional analysis of cell division genes in a developmental context. As part of such an approach, we characterized the *e1466* mutation, which defined the *C. elegans* gene *lin-6* (Horvitz and Sulston, 1980). The *lin-6* mutant phenotype combines absence of DNA replication with continued mitosis, substantial development of the gonad and germline, variable growth and partly penetrant larval lethality. We found that the *lin-6(e1466)* mutation affects the gene *mcm-4*, which encodes the single *C. elegans* MCM-4 subunit of the MCM2-7 replicative helicase. MCM2-7 function has been poorly characterized in *C. elegans*, with *mcm-5(fw7)* as the only other reported mutant (Wang et al., 2007). Many aspects of the *mcm-4(e1466)* phenotype agree with a function as an MCM2-7 subunit, as determined in other systems. However, the tissue-specific effects of *mcm-4* inactivation are surprising for a basic component of the DNA replication machinery.

mcm-4 plays a key role in DNA replication and the replication checkpoint, but mutants continue gonad development

The absence of DNA synthesis in *mcm-4* mutants is consistent with the critical function of MCM-4 in DNA replication licensing and origin unwinding (Aparicio et al., 1997; Ying and Gautier, 2005; You et al., 1999). However, in *mcm-4* mutants DNA replication and cell division continue in the germline during larval development, even allowing the formation of sperm. We expect that perdurance of maternal product and a strong checkpoint response permit continued division cycles in the *mcm-4* gonad. The precursors of the somatic gonad and germline (Z1/Z4 and Z2/Z3, respectively) are formed and set aside in early embryogenesis (Sulston et al., 1983). Hence, Z1-Z4 might use residual maternal product to continue replication in larval development. Similarly, *cyd-1* and *cdk-4* mutants show fully penetrant arrest of postembryonic somatic blast cell divisions, while some divisions of the gonadal precursors continue (Boxem and van den Heuvel, 2001; Park and Krause, 1999). At the same time, gonad development in *mcm-4* mutants is severely retarded compared to that of the wild type. We expect that this difference reflects a gradual decrease in the number of active replication origins. In *Xenopus*, it has been estimated that 10–20 times more MCM2-7 molecules are loaded onto DNA in G1 than the number of origins that are used for DNA replication (see (Edwards et al., 2002; Takahashi et al., 2005). This excess of MCM proteins is expected to license origins that are normally dormant, but allow full DNA synthesis during replicative or genotoxic stress (Ibarra et al., 2008; Woodward et al., 2006). This process is likely to play a role in *C. elegans* replication control as well. Partial inactivation of
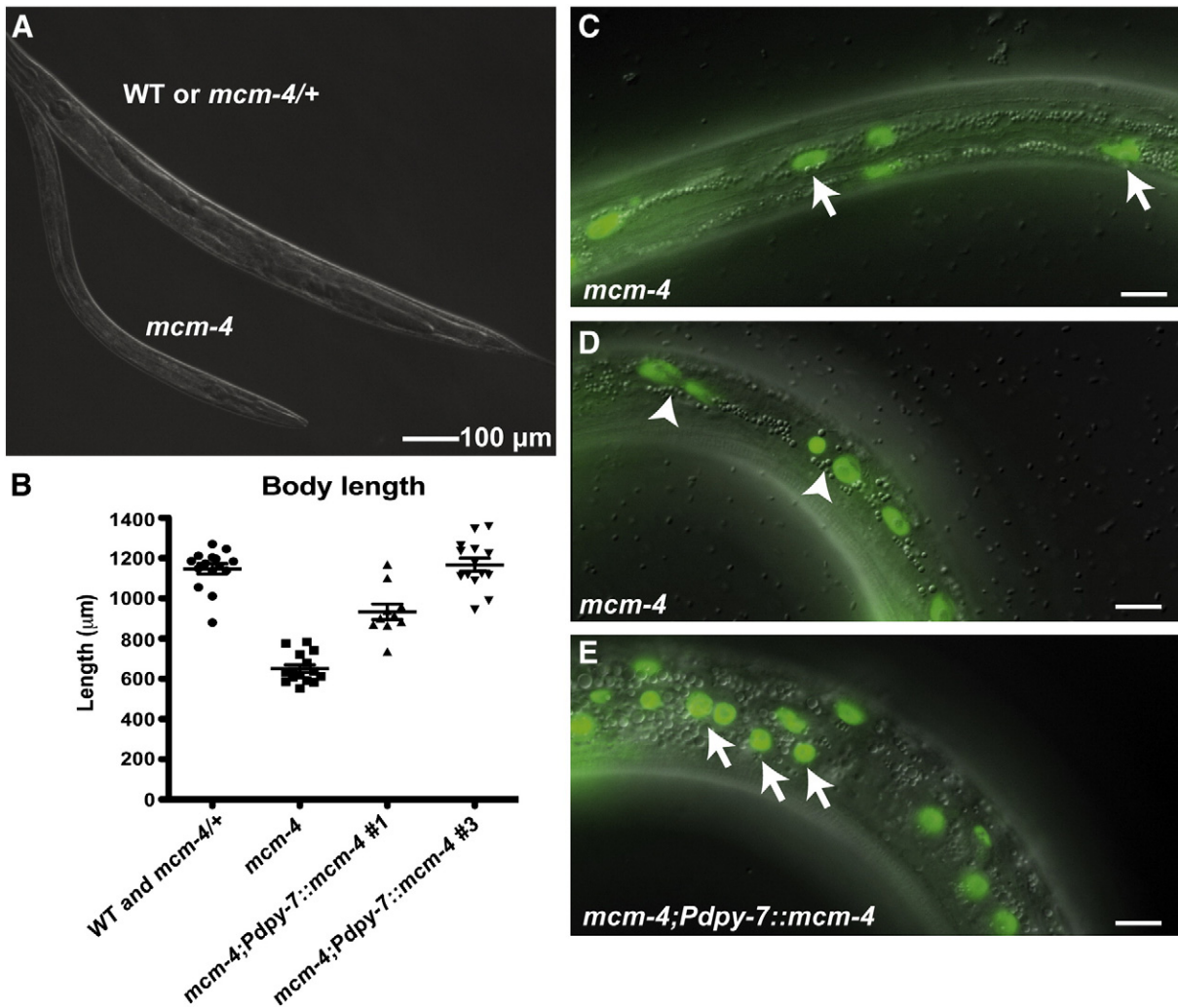
Fig. 7. Epidermal expression of MCM-4 rescues the growth defect of *mcm-4* mutants. Mutant *mcm-4* larvae are severely growth retarded. A: Light micrograph shows comparison between a heterozygous *mcm-4(e1466)/+* adult animal and homozygous *mcm-4(e1466)* animal of the same age, and B. Quantification of the growth defect of adult *mcm-4* animals. Dots represent individual animals. Horizontal lines indicate average ± SEM. C–E. Combined DIC and fluorescence images of *mcm-4* mutant animals carrying an extrachromosomal *Psur-5::GFP* reporter, which marks all nuclei (green). In (E), the array also contains a *Pdpy-7::MCM-4::mCherry* rescue construct, which is expressed in the epidermis and weakly in posterior P cell descendants (A. Saffer and H.R. Horvitz, personal communication). The epidermis of *mcm-4* mutant animals contains few nuclei (C, arrows), which often show signs of aberrant mitosis (D, arrowheads). Mutants carrying the *Pdpy-7::MCM-4::mCherry* construct have additional epidermal nuclei (E, arrows) as well as an increased body size compared to *mcm-4* mutant animals without the construct. (E, compare with C,D, quantification in B).

C. elegans MCM proteins by RNAi makes animals hypersensitive to an otherwise non-inhibitory dose of HU (Woodward et al., 2006). Because of the normal excess of MCM proteins, depletion of maternal MCM-4 pools might not be harmful for several rounds of replication, in particular if the time in S phase can be extended through a checkpoint that monitors the completion of DNA synthesis. We expect that the presence of a robust S-phase checkpoint response in the germline (Gartner et al., 2000) contributes to the continued replication with limiting amounts of MCM-4.

Our data show that MCM-4 is required for replication checkpoint activation in somatic cells. During larval development of *mcm-4* mutants, somatic blast cells entered mitosis without delay and independent of the presence of HU. In addition, divisions in *mcm-4 (RNAi)* embryos continued without DNA replication, resulting in a fragmented genome. These results agree with studies of other organisms, which clarified the requirement of the MCM complex in activation of the DNA damage and replication checkpoints. Critical in checkpoint activation is the recruitment of Replication Protein A (RPA) to single-stranded DNA (Zou and Elledge, 2003). The helicase activity of MCM proteins generates ssDNA, through unwinding the DNA at the replication fork. When replication forks are stalled, e.g.

because of treatment with HU, the MCM helicase activity becomes uncoupled from DNA polymerase activity (Byun et al., 2005). Consequently, fork stalling leads to an accumulation of ssDNA, which recruits additional RPA and causes activation of the checkpoint kinases ATR and Chk1. Both replication fork formation and ssDNA generation require MCM4 function; when MCM4 function is absent, DNA synthesis cannot initiate and the replication checkpoint cannot be activated.

MCM-4 is dynamically regulated throughout the cell cycle and development

In agreement with observations of other eukaryotes, our data indicate that DNA licensing takes place in late M phase and possibly continues in G1. MCM-4 started to co-localize with the DNA in late anaphase in both embryonic and larval cell divisions (Figs. 5 and 6 and Fig. S5). However, upon temporary arrest of cell division or terminal differentiation MCM-4 decreased below detection by immunostaining or MCM-4::mCherry fluorescence. In contrast, Western blotting experiments showed reduced but clearly detectable MCM-4 levels in arrested L1 animals and dauer larvae (Fig. 6). Thus, a relatively low amount of origin-bound MCM2-7 might drive DNA synthesis in cells

that exit from arrest. Alternatively, MCM proteins newly synthesized in G1 might carry out this function.

We observed strong induction of MCM-4 expression around the time of S-phase onset. The transcription of MCM2-7 genes is inhibited by *lin-35* Rb together with E2F transcription factors and activated by CYD-1/CDK-4 and CYE-1/CDK-2 cyclin/CDK complexes (J.K, and S.v.d. H, in preparation, (Kirienko and Fay, 2007). Thus, MCM expression is likely induced at the G1/S transition, close to the switch from origin licensing to origin firing. An important question is whether the newly synthesized MCM-4 can contribute origin-licensing and helicase activities immediately in S phase, while origin re-firing is prevented. In mammalian cells released from quiescence, MCM loading has been shown to occur in late G1 (Mukherjee et al., 2009). Cdt1 and Cdc6 are essential loading factors for the MCM2-7 complex in various eukaryotes, and their inactivation prevents origin re-firing during S phase (Arias and Walter, 2007). The *C. elegans* orthologs CDT-1 and CDC-6 are both inactivated during S phase in a DNA replication and CUL-4/DDB-1 E3 ubiquitin ligase-dependent manner (Kim et al., 2007; Kim and Kipreos, 2007; Korzelius and van den Heuvel, 2007; Zhong et al., 2003). Thus, MCM proteins expressed in late G1 might contribute to a single round of origin firing, as determined by CDT-1 and CDC-6 availability.

Loss of mcm-4 reveals a remarkable uncoupling between cell cycle progression and organismal development and growth

One of the striking aspects of the *mcm-4* phenotype is that it exposes an uncoupling between cell cycle progression and developmental processes such as differentiation. During cell cycle progression, checkpoints ensure that earlier events are completed before later events initiate. Such feedback mechanisms do not appear to exist for cell division and cell fate acquisition. Based on reporter gene expression and cell morphology, successful mitosis is not needed for induction of subsequent S phases or induction of differentiation (Fig. 3 and Figs. S1 and S2). In this light, it is surprising that growth, which can occur quite independently of cell division (Grewal and Edgar, 2003), was severely retarded in *mcm-4* mutants. Furthermore, *mcm-4* mutant animals frequently died during the larval molt. *cyd-1* and *cdk-4* mutants also lack DNA replication and grow slowly, but these mutants do not display any larval lethality (Boxem and van den Heuvel, 2001). Thus, the continued mitosis in the absence of DNA replication, which is specific for *mcm-4* mutants, might cause the reduced viability.

Surprisingly, *mcm-4* function in the epidermis was sufficient for normal viability and restored larval growth to wild-type levels. In *C. elegans*, only the intestine and epidermis undergo rounds of endoreduplication during larval development (Hedgecock and White, 1985). A positive correlation between ploidy of the *C. elegans* epidermis and volume of the adult animal has provided a strong argument for growth control by endoreduplication (Flemming et al., 2000; Lozano et al., 2006). Intestinal expression of MCM-4 restored DNA replication and nuclear division in *mcm-4* larvae but did not rescue the growth and viability defects. In contrast, epidermal expression of MCM-4 rescued the larval lethality as well as the reduced length and thin appearance of *mcm-4* mutants. As lethality coincides with the molt, *mcm-4* mutants might die from reduced integrity of the cuticle. Expression of *mcm-4* in the epidermis of *mcm-4* mutants prevents the loss of seam cells that normally contribute to cuticle formation (Fig. S7B; (see Fritz and Behm, 2009 and references therein). Moreover, *mcm-4* expression in the syncytial epidermis restores endoreduplication, which may promote growth as well as cuticle secretion.

DBL-1 TGFβ has been shown to control postembryonic growth through regulation of SMA-3 in the epidermis (Wang et al., 2002). This effect has been linked to the control of DNA replication (Lozano et al., 2006; Wang et al., 2002). *cye-1*, *cyd-1* and *cdk-4* mutants all show reduced growth, in contrast to *cdk-1* mutants that arrest cell division in G2 (Boxem et al., 1999; Boxem and van den Heuvel, 2001;

Lozano et al., 2006). In particular, the *cye-1* G1 cyclin was found to be crucial for epidermal polyploidization (Lozano et al., 2006). Further studies will be needed to determine if the DBL-1 TGFβ/SMA-3 pathway induces G1 cyclin expression to promote DNA replication and growth of the animal.

Taken together, our findings highlight a remarkable independence among DNA replication, differentiation and cell cycle progression. In addition, our results show that a component of the basic DNA replication machinery can have distinct tissue-specific requirements in growth and viability, which makes it a potential target for regulation by developmental control pathways.

Supplementary materials related to this article can be found online at doi:10.1016/j.ydbio.2010.12.009.

References

Aparicio, O.M., Weinstein, D.M., Bell, S.P., 1997. Components and dynamics of DNA replication complexes in *S. cerevisiae*: redistribution of MCM proteins and Cdc45p during S phase. Cell 91, 59–69.

Arias, E.E., Walter, J.C., 2006. PCNA functions as a molecular platform to trigger Cdt1 destruction and prevent re-replication. Nat. Cell Biol. 8, 84–90.

Arias, E.E., Walter, J.C., 2007. Strength in numbers: preventing rereplication via multiple mechanisms in eukaryotic cells. Genes Dev. 21, 497–518.

Bell, S.P., Dutta, A., 2002. DNA replication in eukaryotic cells. Annu. Rev. Biochem. 71, 333–374.

Boxem, M., van den Heuvel, S., 2001. *lin-35* Rb and *cki-1* Cip/Kip cooperate in developmental regulation of G1 progression in *C. elegans*. Development 128, 4349–4359.

Boxem, M., Srinivasan, D.G., van den Heuvel, S., 1999. The *Caenorhabditis elegans* gene *ncc-1* encodes a *cdc2*-related kinase required for M phase in meiotic and mitotic cell divisions, but not for S phase. Development 126, 2227–2239.

Brauchle, M., Baumer, K., Gonczy, P., 2003. Differential activation of the DNA replication checkpoint contributes to asynchrony of cell division in *C. elegans* embryos. Curr. Biol. 13, 819–827.

Byun, T.S., Pacek, M., Yee, M.C., Walter, J.C., Cimprich, K.A., 2005. Functional uncoupling of MCM helicase and DNA polymerase activities activates the ATR-dependent checkpoint. Genes Dev. 19, 1040–1052.

Ciccia, A., Elledge, S.J., 2010. The DNA damage response: making it safe to play with knives. Mol. Cell 40, 179–204.

Claycomb, J.M., Orr-Weaver, T.L., 2005. Developmental gene amplification: insights into DNA replication and gene expression. Trends Genet. 21, 149–162.

Edgar, B.A., Orr-Weaver, T.L., 2001. Endoreplication cell cycles: more for less. Cell 105, 297–306.

Edwards, M.C., Tutter, A.V., Cvetic, C., Gilbert, C.H., Prokhorova, T.A., Walter, J.C., 2002. MCM2-7 complexes bind chromatin in a distributed pattern surrounding the origin recognition complex in *Xenopus* egg extracts. J. Biol. Chem. 277, 33049–33057.

Encalada, S.E., Martin, P.R., Phillips, J.B., Lyczak, R., Hamill, D.R., Swan, K.A., Bowerman, B., 2000. DNA replication defects delay cell division and disrupt cell polarity in early *Caenorhabditis elegans* embryos. Dev. Biol. 228, 225–238.

Flemming, A.J., Shen, Z.Z., Cunha, A., Emmons, S.W., Leroi, A.M., 2000. Somatic polyploidization and cellular proliferation drive body size evolution in nematodes. Proc. Natl Acad. Sci. USA 97, 5285–5290.

Fogarty, P., Campbell, S.D., Abu-Shumays, R., Phalle, B.S., Yu, K.R., Uy, G.L., Goldberg, M.L., Sullivan, W., 1997. The *Drosophila* grapes gene is related to checkpoint gene chk1/ rad27 and is required for late syncytial division fidelity. Curr. Biol. 7, 418–426.

Francis, R., Waterston, R.H., 1991. Muscle cell attachment in Caenorhabditis elegans. J. Cell Biol. 114, 465–479.

Fritz, J.A., Behm, C.A., 2009. CUTI-1: a novel tetraspan protein involved in C. elegans CUTicle formation and epithelial integrity. PLoS ONE 4, e5117.

Gartner, A., Milstein, S., Ahmed, S., Hodgkin, J., Hengartner, M.O., 2000. A conserved checkpoint pathway mediates DNA damage-induced apoptosis and cell cycle arrest in C. elegans. Mol. Cell 5, 435–443.

Grewal, S.S., Edgar, B.A., 2003. Controlling cell division in yeast and animals: does size matter? J. Biol. 2, 5.

Hawkins, M.G., McGhee, J.D., 1995. elt-2, a second GATA factor from the nematode *Caenorhabditis elegans*. J. Biol. Chem. 270, 14666–14671.

Hedgecock, E.M., White, J.G., 1985. Polyploid tissues in the nematode *Caenorhabditis elegans*. Dev. Biol. 107, 128–133.

Hook, S.S., Lin, J.J., Dutta, A., 2007. Mechanisms to control rereplication and implications for cancer. Curr. Opin. Cell Biol. 19, 663–671.

Horvitz, H.R., Sulston, J.E., 1980. Isolation and genetic characterization of cell-lineage mutants of the nematode *Caenorhabditis elegans*. Genetics 96, 435–454.

Ibarra, A., Schwob, E., Mendez, J., 2008. Excess MCM proteins protect human cells from replicative stress by licensing backup origins of replication. Proc. Natl Acad. Sci. USA 105, 8956–8961.

Kim, Y., Kipreos, E.T., 2007. The *Caenorhabditis elegans* replication licensing factor CDT-1 is targeted for degradation by the CUL-4/DDB-1 complex. Mol. Cell. Biol. 27, 1394–1406.

Kim, J., Feng, H., Kipreos, E.T., 2007. *C. elegans* CUL-4 prevents rereplication by promoting the nuclear export of CDC-6 via a CKI-1-dependent pathway. Curr. Biol. 17, 966–972.

Kipreos, E.T., 2005. *C. elegans* cell cycles: invariance and stem cell divisions. Nat. Rev. Mol. Cell Biol. 6, 766–776.

Kirienko, N.V., Fay, D.S., 2007. Transcriptome profiling of the *C. elegans* Rb ortholog reveals diverse developmental roles. Dev. Biol. 305, 674–684.

Korzelius, J., van den Heuvel, S., 2007. Replication licensing: oops! ... I did it again. Curr. Biol. 17, R630–R632.

Labib, K., Tercero, J.A., Diffley, J.F., 2000. Uninterrupted MCM2-7 function required for DNA replication fork progression. Science 288, 1643–1647.

Lilly, M.A., Duronio, R.J., 2005. New insights into cell cycle control from the Drosophila endocycle. Oncogene 24, 2765–2775.

Lozano, E., Saez, A.G., Flemming, A.J., Cunha, A., Leroi, A.M., 2006. Regulation of growth by ploidy in *Caenorhabditis elegans*. Curr. Biol. 16, 493–498.

Mello, C.C., Kramer, J.M., Stinchcomb, D., Ambros, V., 1991. Efficient gene transfer in *C. elegans*: extrachromosomal maintenance and integration of transforming sequences. EMBO J. 10, 3959–3970.

Mukherjee, P., Cao, T.V., Winter, S.L., Alexandrow, M.G., 2009. Mammalian MCM loading in late-G(1) coincides with Rb hyperphosphorylation and the transition to post-transcriptional control of progression into S-phase. PLoS ONE 4, e5462.

Nass, R., Hall, D.H., Miller III, D.M., Blakely, R.D., 2002. Neurotoxin-induced degeneration of dopamine neurons in *Caenorhabditis elegans*. Proc. Natl Acad. Sci. USA 99, 3264–3269.

Nguyen, V.Q., Co, C., Li, J.J., 2001. Cyclin-dependent kinases prevent DNA re-replication through multiple mechanisms. Nature 411, 1068–1073.

O'Neil, N., Rose, A., 2006. DNA repair. WormBook 1–12.

Pacek, M., Walter, J.C., 2004. A requirement for MCM7 and Cdc45 in chromosome unwinding during eukaryotic DNA replication. EMBO J. 23, 3667–3676.

Park, M., Krause, M.W., 1999. Regulation of postembryonic G(1) cell cycle progression in *Caenorhabditis elegans* by a cyclin D/CDK-like complex. Development 126, 4849–4860.

Petersen, B.O., Lukas, J., Sorensen, C.S., Bartek, J., Helin, K., 1999. Phosphorylation of mammalian CDC6 by Cyclin A/CDK2 regulates its subcellular localization. EMBO J. 18, 396–410.

Piatti, S., Bohm, T., Cocker, J.H., Diffley, J.F., Nasmyth, K., 1996. Activation of S-phase-promoting CDKs in late G1 defines a "point of no return" after which Cdc6 synthesis cannot promote DNA replication in yeast. Genes Dev. 10, 1516–1531.

Schwob, E., Nasmyth, K., 1993. *CLB5* and *CLB6*, a new pair of B cyclins involved in DNA replication in *Saccharomyces cerevisiae*. Genes Dev. 7, 1160–1175.

Senga, T., Sivaprasad, U., Zhu, W., Park, J.H., Arias, E.E., Walter, J.C., Dutta, A., 2006. PCNA is a cofactor for Cdt1 degradation by CUL4/DDB1-mediated N-terminal ubiquitination. J. Biol. Chem. 281, 6246–6252.

Sibon, O.C., Stevenson, V.A., Theurkauf, W.E., 1997. DNA-replication checkpoint control at the *Drosophila* midblastula transition. Nature 388, 93–97.

Strome, S., Wood, W.B., 1983. Generation of asymmetry and segregation of germ-line granules in early C. elegans embryos. Cell 35, 15–25.

Sulston, J.E., Horvitz, H.R., 1981. Abnormal cell lineages in mutants of the nematode *Caenorhabditis elegans*. Dev. Biol. 82, 41–55.

Sulston, J.E., Schierenberg, E., White, J.G., Thomson, J.N., 1983. The embryonic cell lineage of the nematode *Caenorhabditis elegans*. Dev. Biol. 100, 64–119.

Takahashi, T.S., Wigley, D.B., Walter, J.C., 2005. Pumps, paradoxes and ploughshares: mechanism of the MCM2-7 DNA helicase. Trends Biochem. Sci. 30, 437–444.

van den Heuvel, S., 2005. Cell-cycle regulation. WormBook 1–16.

van der Voet, M., Lorson, M.A., Srinivasan, D.G., Bennett, K.L., van den Heuvel, S., 2009. *C. elegans* mitotic cyclins have distinct as well as overlapping functions in chromosome segregation. Cell Cycle 8.

Wang, J., Tokarz, R., Savage-Dunn, C., 2002. The expression of TGFbeta signal transducers in the hypodermis regulates body size in *C. elegans*. Development 129, 4989–4998.

Wang, X., Suh, C., Zhu, Z., Fan, Q., 2007. Minichromosome maintenance protein 5 homologue in Caenorhabditis elegans plays essential role for postembryonic development. Biochem. Biophys. Res. Commun. 359, 965–971.

Woodward, A.M., Gohler, T., Luciani, M.G., Oehlmann, M., Ge, X., Gartner, A., Jackson, D.A., Blow, J.J., 2006. Excess Mcm2-7 license dormant origins of replication that can be used under conditions of replicative stress. J. Cell Biol. 173, 673–683.

Ying, C.Y., Gautier, J., 2005. The ATPase activity of MCM2-7 is dispensable for pre-RC assembly but is required for DNA unwinding. EMBO J. 24, 4334–4344.

You, Z., Komamura, Y., Ishimi, Y., 1999. Biochemical analysis of the intrinsic Mcm4-Mcm6-mcm7 DNA helicase activity. Mol. Cell. Biol. 19, 8003–8015.

Zhong, W., Feng, H., Santiago, F.E., Kipreos, E.T., 2003. CUL-4 ubiquitin ligase maintains genome stability by restraining DNA-replication licensing. Nature 423, 885–889.

Zou, L., Elledge, S.J., 2003. Sensing DNA damage through ATRIP recognition of RPA-ssDNA complexes. Science 300, 1542–1548.